RSC Advances

# Surface Plasmon-Enhanced Dye-Sensitized Solar Cells Based on Double-Layered Composite Films Consisting of TiO2/Ag and TiO2/Au Nanoparticles


| | |
|---|---|
| Journal: | *RSC Advances* |
| Manuscript ID: | RA-ART-03-2015-003677 |
| Article Type: | Paper |
| Date Submitted by the Author: | 02-Mar-2015 |
| Complete List of Authors: | Kim, Hyun-Young; Seoul National University,<br>Song, Da Hyun; Seoul National University,<br>Yoon, Hyeokjin; Seoul National University, Chemistry<br>Suh, Jung Sang; Seoul National University, Chemistry |
| | |

Journal Name

RSCPublishing

ARTICLE

# Surface Plasmon-Enhanced Dye-Sensitized Solar Cells Based on Double-Layered Composite Films Consisting of $TiO_2$/Ag and $TiO_2$/Au Nanoparticles

Hyun-Young Kim [1], Da Hyun Song[1], Hyeokjin Yoon, and Jung Sang Suh*,

Cite this: DOI: 10.1039/x0xx00000x

Received 00th January 2012,
Accepted 00th January 2012

DOI: 10.1039/x0xx00000x

www.rsc.org/

We have fabricated silver and gold colloid particles, and used them to fabricate surface plasmon-enhanced dye-sensitized solar cells (DSSCs) based on N719 dye. N719 dye, which is the most heavily used dye in DSSCs, has two strong visible absorption bands centered at 393 and 533 nm. The localized surface plasmon absorption band of Ag nanoparticles (NPs) was well matched with the higher energy band of N719 dye, while that of Au NPs with the lower one. The energy conversion efficiency was significantly improved from the DSSCs based on double-layered composite films; the bottom layer consisted of $TiO_2$ and Ag NPS, while the top one consisted of $TiO_2$ and Au NPs. The efficiency was 10.0%, which was almost the same as the highest value reported on the surface plasmon-enhanced DSSCs. The high efficiency might be due to a good energy matching between the extinction bands of Ag and Au NPs and absorption bands of N719 dye.

## Introduction

Diverse optical properties of metal nanoparticles (NPs) like silver and gold are generated mainly by their localized surface plasmon resonances (LSPRs).[1] LSPRs are excited when the frequency of light photons matches the natural frequency of the collective oscillation of conduction electrons in metal NPs. LSPRs create sharp spectral absorption and scattering peaks as well as strong electromagnetic near-field enhancements.[1] One of the most interesting features of LSPRs is an enhanced light absorption of molecules that are adsorbed on noble NPs like silver or gold.[2] The principle of LSPRs has been applied to increase the optical absorption and/or photocurrent in a wide range of solar cell configurations.[3-20]

Dye-sensitized solar cells (DSSCs) have received much attention due to the high energy conversion efficiency and low cost.[21-24] Localized surface plasmon-enhanced DSSCs are based on the fact that the light absorption of dye molecules adsorbed on noble metal nanoparticles (NPs) like silver or gold is enhanced.[2,3] The energy conversion efficiency of DSSCs based on N719 dye has been improved significantly by adapting core-shell Au NPs.[25,26] The highest efficiency reported on the surface plasmon-enhanced DSSCs is 10.2%.[26] Silver sol has yellow colour and its localized surface plasmon absorption takes place near 390 nm, while gold sol has red colour and its plasmon absorption near 530 nm. N719 dye is the most heavily used dye in DSSCs. It has two strong visible absorption bands centered at 393 and 533 nm. The lower energy band of N719 dye is well matched with the localized surface plasmon absorption band of gold NPs, while the higher energy band with that of silver NPs. Therefore, one could maximize the plasmon-enhanced absorption of N719 dye by including Ag and Au NPs together in the fabrication of DSSCs. Here, we have studied the efficiency of the DSSCs based on double-layer composite films consisting of $TiO_2$/Ag and $TiO_2$/Au NPs.

## Experimental Section

**Preparation of spherical Ag NPs.** Ag seed solution was prepared by following proceeds: 0.30 mL of 10 mM silver nitrate solution and 20 mL of 1 mM trisodium citrate solution were mixed together. To this solution, 1.8 mL of ice-cold 10 mM sodium borohydride was rapidly injected and mixture stirred vigorously. The whole solution was aged for 3 h at room temperature. 9 mL of the Ag seed solution, 11 mL of water and 1.2 mL of 20 mM ascorbic acid solution were mixed together. To this solution, 1.2 mL of 10 mM silver nitrate solution was rapidly injected and mixture stirred vigorously. Spherical Ag NPs with an average size of 29 nm were made.

**Preparation of spherical Au NPs.** Au spheres were prepared following previously reported method.[27] 50 mL of 0.5 mM $HAuCl_4$ was heated at 90°C for 1h. When boiling the solution, 300 $\mu$L of sodium citrate solution (1%) was added to the solution. After stirring

for 30 min at 90°C, spherical Au NPs with an average size of 33 nm were obtained.

**Fabrication of DSSCs.** A $TiO_2$ blocking layer was formed on cleaned FTO (fluorine-doped thin oxide) glass by spin-coating with 5 wt% of titanium di-isopropoxide bis(acetylacetonate) in butanol and annealed at 450 ºC for 1 h. The photoanodes incorporated with metal (Ag or Au) NPs and $TiO_2$ NP paste (ratio of metal NPs to $TiO_2$ NPs is from 0 to 1.5 wt%) were prepared using the following procedure: controlled amount of metal NPs were mixed with $TiO_2$ NP paste (T/SP, solaronix) in methyl alcohol, followed by stirring and sonication, and then the solvent was evaporated in vacuum. The $TiO_2$ NP paste or sets of $TiO_2$ NP pastes containing metal NPs were coated onto the FTO glass by the doctor blade technique, and then heated gradually at 450 ºC for 1 h. A paste for the scattering layer (DSL 18NR-AO, Dyesol) was coated by doctor blade and then dried for 2h at 50 °C. The resulting films were treated in titanium isopropoxide (TIP) solutions (0.1 M in isopropyl alcohol) for 30 min at 90 ºC, and followed by annealing at 450 ºC for 30 min. The metal-$TiO_2$ films or $TiO_2$ films were immersed into a N719 (Solaronix) dye or black dye solution in ethanol under heating to 50 ºC for 12 h. Pt-layered counter-electrodes were prepared by spin-coating $H_2PtCl_6$ solution (0.5 M in EtOH) onto FTO glass and then sintered at 400 ºC for 30 min. The photoanode was further sandwiched by Pt-coated FTO glass, by using a 60 µm - thick surlyn. The composition of the electrolyte was as follows: 0.7 M of 1 butyl -3-methyl imidazolium iodide (BMII), 0.03 M of $I_2$, 0.1 M of guanidium thiocyanate (GSCN), and 0.5 M of 4 *tert*-butyl pyridine (TBP) in a mixture of acetonitrile and valeronitrile (85: 15 *v/v*).

**Characterization of metal NPs and DSSCs.** The geometry and size of metal NPs were confirmed by an energy-filtering transmittance electron microscope (EF-TEM, Carl Zeiss, LIBRA 120). Energy dispersive spectroscopy (EDS) analysis of double layered DSSCs based on Au NPs/$TiO_2$ and Ag NPs/$TiO_2$ was done by using a field emission scanning electron microscope(FE-SEM, JSM-6330F, JEOL Inc.). Current density-voltage (*J-V*) characteristics of the DSSCs were measured using an electrometer (KEITHLEY 2400) under AM 1.5 illumination (100 mW/cm$^2$) provided by a solar simulator (1 KW xenon with AM 1.5 filter, PEC-L01, Peccel Technologies). The incident photon-to-current conversion efficiency (IPCE) was measured using McScience (model K3100) with reference to the calibrated diode. A 300 W Xenon lamp was used as light source for generation of a monochromatic beam. The bias light was supplied by a 150 W halogen lamp. The spectra of the electrochemical impedance spectroscopy (EIS) were measured with a potentiostat (Solartron 1287) equipped with a frequency response analyzer (Solartron 1260), with the frequency ranging from $10^{-1}$ to $10^5$ Hz. The applied bias voltage and ac amplitude were set at open circuit voltage ($V_{oc}$) of the DSSCs and 10 mV, respectively. The impedance measurements were carried out at open-circuit potential under AM 1.5 one-sun light illumination.

## Results and Discussion

Figure 1 shows the UV-visible extinction spectra of silver and gold sols and the TEM images of their colloidal NPs. For comparison, the UV-visible absorption spectrum of N719 dye is also shown. The extinction maximum of silver sol is near 390 nm, while that of gold sol is near 530 nm. These bands are well matched with two visible absorption bands of N719 dye centered at 393 and 533 nm. The average size of colloidal silver NPs is about 29 nm, while that of colloidal gold NPs is 33 nm.

The photocurrent density-voltage (*J-V*) curves were measured in air mass 1.5 sunlight from the DSSCs based on N719 dye and composite films consisting of $TiO_2$ and Ag or Au NPs. All the films were pretreated with TIP. It should be mentioned that bare metal NPs could have direct contact with the dye and the electrolyte. In this case, the recombination and back reaction of photogenerated carriers can take place.[2] In order to overcome these problems, core-shell NPs, in which the surfaces of metal NPs are protected with an insulator or semiconductor, have been adapted.[25,26] It is known that by pretreating with TIP, the surface of metal NPs is coated with $TiO_2$.[28] The dependence of the energy conversion efficiency ($\eta$) and short-circuit current density ($J_{sc}$) of plasmon-enhanced DSSCs on Ag or Au NPs weight percent was investigated. Ag NPs whose average size was 29 nm were used in fabrication of the DSCCs based on the composite films consisting of $TiO_2$ and Ag NPs, while 33 nm Au NPs in fabrication of those consisting of $TiO_2$ and Au NPs. Figure 2(a) shows the dependence of 29 nm Ag NPs weight percent on $\eta$ and $J_{sc}$ values measured from $TiO_2$/Ag DSSCs. As the weight

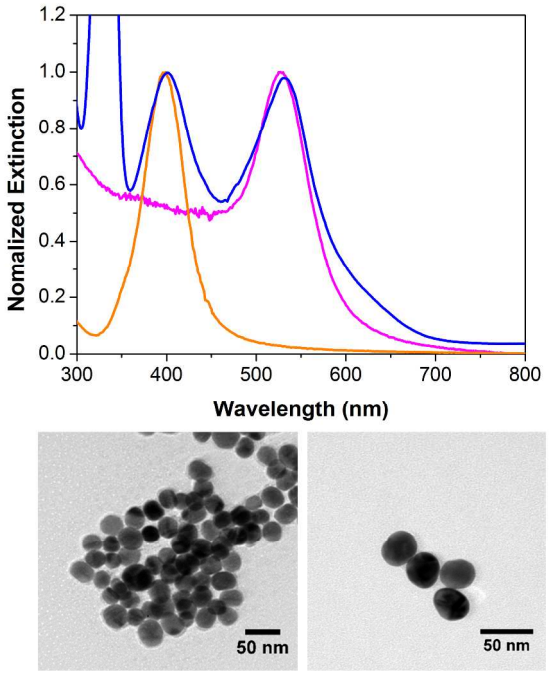


**Fig 1.** (Top) UV-visible absorption spectrum of N719 dye (blue) and extinction spectra of silver (orange) and gold (pink) sols, and (bottom) the TEM images of colloidal silver (left) and gold (right) NPs. The average size of colloidal silver and gold NPs is about 29 and 33 nm, respectively.

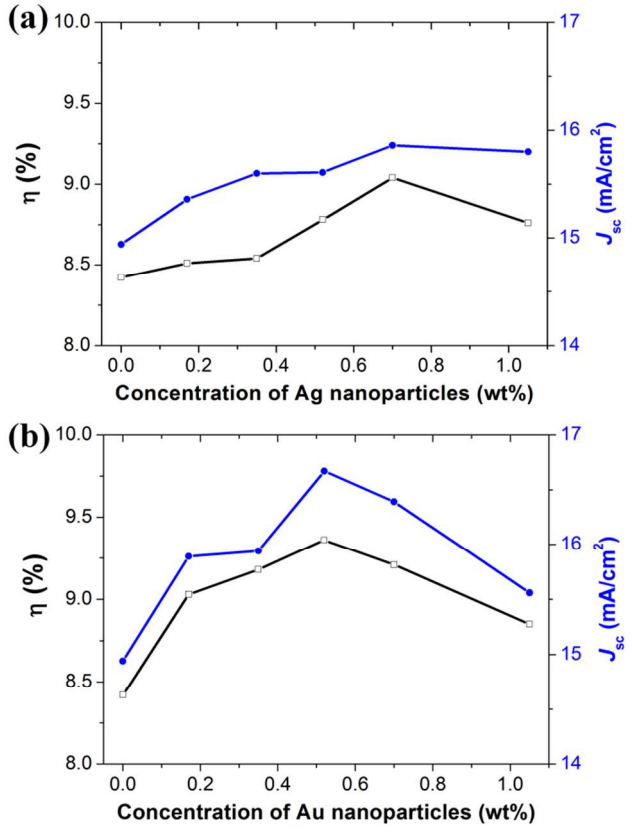


**Fig 2.** Dependence of metal NPs weight percent on $\eta$ and $J_{sc}$ values measured from the DSSCs based on (a) $TiO_2$ and Ag NPs film and (b) $TiO_2$ and Au NPs film. The average size of Ag and Au NPs included in the fabrication of the DSSCs was 29 and 33 nm, respectively.

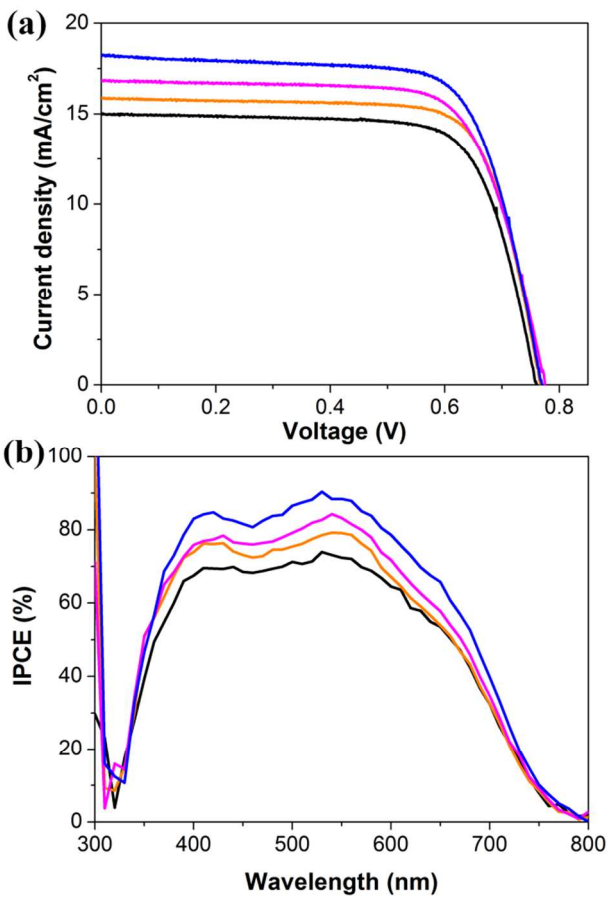


**Fig 3.** Photocurrent density-voltage (*J-V*) curves (a) and IPCE spectra (b) measured from the DSSCs based on $TiO_2$ film (black), $TiO_2$/Ag NPs film (orange), $TiO_2$/Au NPs film (red), and double-layered film consisting of $TiO_2$/Au NPs and $TiO_2$/Ag NPs (blue). All the films were pretreated with TIP.

percent of 29 nm Ag NPs was raised up to 0.70 wt%, the $\eta$ value was gradually increased from 8.42% up to the maximum value, 9.04%. Further increase in the weight percent of Ag NPs to 1.05 wt% actually caused a decrease in the $\eta$ values to 8.76%. A trend observed from the change in the energy conversion efficiency was found to be in agreement with that from a change in the photocurrent density. The $J_{sc}$ value was enhanced from 14.94 to 15.86 mA/cm$^2$ as the weight percent of Ag NPs approached 0.70 wt%, and a further increase of Ag weight percent led to a slow decrease in $\eta$ and $J_{sc}$. Figure 2(b) shows the dependence of 33 nm Au NPs weight percent on $\eta$ and $J_{sc}$ values measured from $TiO_2$/Au DSSCs. For 33 nm Au NPs, the highest $\eta$ value, 9.36%, was obtained when the weight percent of Au NPs was 0.52 wt%. A further increase of Au weight percent led to a steep decrease in $\eta$ and $J_{sc}$.

Figure 3 shows the photocurrent density-voltage (*J-V*) curves (a) and IPCE spectra (b) measured from the DSSCs based on the film of only $TiO_2$ NPs, composite film of $TiO_2$ and Ag NPs, composite film of $TiO_2$ and Au NPs, and double-layered film. For the double-layered film, the composite layer consisting of $TiO_2$ and 29 nm Ag NPs was under that of $TiO_2$ and 33 nm Au NPs (see Figure S1 and 2). The weight percent of 29 nm Ag NPs was 0.70 wt%, which was the optimum value, while that of 33 nm Au NPs was 0.52 wt%. All the films were pretreated with TIP. The photovoltaic parameters are listed in Table 1. By including Ag or Au NPs, the short-circuit current density ($J_{sc}$) is increased substantially, while the open-circuit voltage ($V_{oc}$) and fill factor (*ff*) are not changed significantly. For the double-layered DSSC, the short-circuit current density increased from 14.94 up to 18.17 mA/cm$^2$, which was the highest value. The

**Table 1.** Photovoltaic properties of the DSSCs based on $TiO_2$ film, $TiO_2$/Ag NPs film, $TiO_2$/Au NPs film, and double-layered film consisting of $TiO_2$/Au NPs and $TiO_2$/Ag NPs. All the films were pretreated with TIP.

| | $V_{oc}$ (V) | $J_{sc}$ (mA/cm$^2$) | *ff* (%) | $\eta$ (%) |
|---|---|---|---|---|
| $TiO_2$ film | 0.76 | 14.94 | 0.74 | 8.42 |
| $TiO_2$/Ag composite film | 0.77 | 15.86 | 0.74 | 9.04 |
| $TiO_2$/Au composite film | 0.78 | 16.67 | 0.72 | 9.36 |
| Double-layered film | 0.77 | 18.17 | 0.72 | 10.03 |

energy conversion efficiency ($\eta$) was improved from 8.42 to 10.03%. The energy conversion efficiency of the DSSC based on a double-layered film is higher than that of single layer films. The efficiency of 10.03% is almost the same as the highest value reported on the surface plasmon-enhanced DSSCs.[26] The thickness of $TiO_2$ film, including the scattering layer, was about 19 $\mu$m, while that of $TiO_2$-metal NPs and double-layered films was 14 $\mu$m. The thickness of the photoactive $TiO_2$ film itself was about 10 $\mu$m in the DSSC based on only $TiO_2$ NPs film, while about 5 $\mu$m in the DSSCs based on $TiO_2$-metal NPs and double-layered films.

By incorporating metal NPs, IPCE over the wavelength range 400 to 700 nm is enhanced. The relative intensity of IPCE spectra seems to be related considerably to the spectral overlap between the extinction bands of Ag and Au NPs and absorption bands of N719 dye. For example, the relative intensity near 530 nm is stronger in the spectrum of the DSSC included Au NPs than that included Ag NPs. This could be explained simply if we assume that metal NPs were not aggregated in the fabrication process, since Au NPs have strong surface plasmon absorption near 530 nm, while isolated Ag NPs have almost no absorption in this region. However, metal NPs could be aggregated in the fabrication process of the composite films. The intensity of the DSSC included Ag NPs is significantly higher near 530 nm than that not included metal NPs. This might be due to the contribution of Ag clusters like dimer and trimer. The optimum concentration of Ag in the DSSCs included Ag NPs is 0.70 wt%, while that of Au in the DSSCs included Au NPs is 0.52 wt%. With increasing relative weight percent of metal NPs, the probability of aggregation between metal NPs in the composite films would be increased. It is well known that when Ag NPs are aggregated, the resonance is red-shifted.[29] Dimer of 29 nm Ag NPs had a strong surface plasmon absorption near 530 nm. Since N719 dye has a strong absorption band at 533 nm, the surface plasmon enhanced absorption could take place on or near dimers of Ag NPs. However, the resonance of isolated Au NPs was already near 530 nm, and the resonance of dimers of Au NPs would be in the red region. Therefore, dimers of Au NPs could be scarcely contributed to the efficiency. In Figure 2, one can see that $\eta$ and $J_{sc}$ decrease when the weight percent of Ag and Au NPs increases beyond their optimum concentration. The decreasing slope in $\eta$ and $J_{sc}$ is much steeper for the DSSCs included Au NPs than those included Ag NPs. This may be due to the fact that the surface plasmon-enhanced absorption of N719 dye could take place on dimers of Ag NPs but not on dimers of Au NPs.

The DSSC based on double-layered composite film shows the highest efficiency. The integrated IPCE value showed higher than that from the DSSC without metal NPs by a factor of 1.28. In Table 1, one can see that $J_{sc}$ is significantly enhanced, while $V_{oc}$ and *ff* are changed slightly. The number of dye molecules adsorbed on the double layered film was fewer than that adsorbed on the $TiO_2$ film and the same as that adsorbed on $TiO_2$-metal film, since the thickness of $TiO_2$ film, including the scattering layer, was about 19 $\mu$m, while that of $TiO_2$-metal NPs and double-layered films was 14 $\mu$m. Therefore, it is concluded that a high conversion efficiency of the DSSC based on double-layered composite film is due to an enhanced light absorption of N719 dye through the energy matching

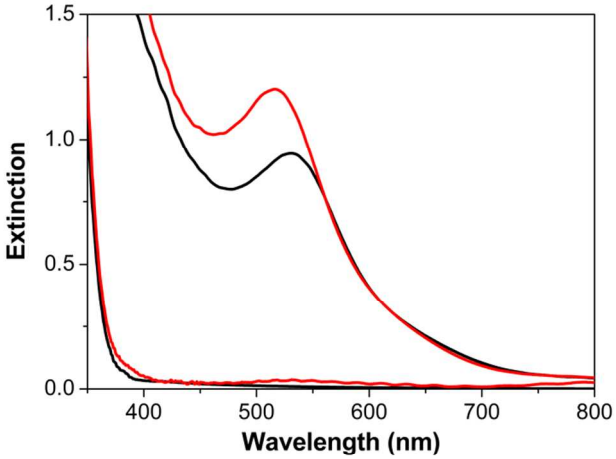


**Fig 4.** Extinction spectra of $TiO_2$ NPs film (black) and double-layered film consisting of $TiO_2$/Au NPs and $TiO_2$/Ag NPs (red) before (bottom two spectra) and after N719 dye adsorption. Both films were treated with TIP before adsorption of dye molecules.

between absorptions of N719 dye and surface plasmon resonances of Ag and Au NPs. One can see the evidence from the change of the extinction spectra of $TiO_2$ NPs film and double-layered film consisting of $TiO_2$/Au NPs and $TiO_2$/Ag NPs before and after N719 dye adsorption (see Figure 4). Before adsorption of dye molecules, there is no significant difference. However, after adsorption of N719 dye molecules, there is a significant difference in intensity. The intensity of the peaks corresponding to the localized surface plasmon resonances of Ag and Au NPs, near 390 and 530 nm, is significantly higher in the extinction spectrum measured from the double-layered film consisting of $TiO_2$/Au NPs and $TiO_2$/Ag NPs than that measured from the $TiO_2$ NPs film. The number of dye molecules adsorbed on both films was almost equal, since the thickness of both films was the same as about 5 $\mu$m. The higher extinction intensity is due to the plasmon effects of metal NPs.

An enhanced light absorption of dye molecules could take place on or near surface of metal NPs and far surface of metal NPs. The LSPRs decay either radiatively (giving rise to dramatic electromagnetic field enhancements, for instance, as used in surface-enhanced Raman spectroscopy) or into (quasi) particles such as electron-hole (e-h) pairs.[1,30] Therefore, the absorption of dye molecules adsorbed on or near the surface of metal NPs could be enhanced greatly by the latter decay path. Also, the absorption of dye molecules, particularly dye molecules apart from the surface of metal NPs, could be enhanced by the strong LSPR scattering of Ag and Au NPs. Since scattering takes place in all directions, the strong LSPR scattering could enhance the absorption of all the dye molecules. The contribution to the efficiency by the strong LSPR scattering of Ag and Au NPs should be studied in detail.

The efficiency of the DSSCs based on double-layered composite films was affected by the geometry of two composite films. With the geometry of the composite layer consisting of $TiO_2$ NPs and 29 nm Ag NPs under that of $TiO_2$ NPs and 33 nm Au NPs, the efficiency was higher than the upside-down geometry (see Table S1). Ag NPs could absorb and scatter much shorter wavelength light than Au NPs,

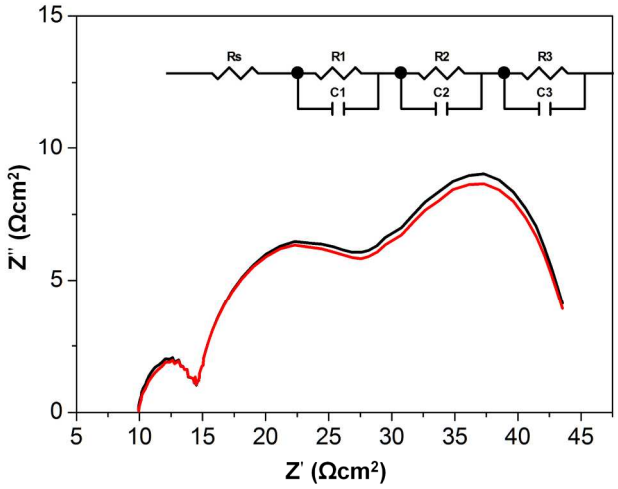


**Fig 5**. Electrochemical impedance spectra of DSSCs based on $TiO_2$ film (black) and double-layered film consisting of $TiO_2$/Au NPs and $TiO_2$/Ag NPs (red). The thickness of the photoactive layer in both cells was about 5 μm.

since the LSPR of Ag NPs is centered at 390 nm, while that of Au NPs at 530 nm. The weight percent of Ag or Au NPs to the $TiO_2$ NPs is less than 1%, and $TiO_2$ NPs are the dominant species. Therefore, the incident light may be reduced mostly by the scattering of $TiO_2$ NPs, since $TiO_2$ NPs have no absorption in visible. With increasing the pass length, relative loss of shorter wavelength light is greater than that of longer wavelength light. Therefore, a better efficiency might be achieved from the DSSC whose composite film included Ag NPs, which absorb and scatter much shorter wavelength light than Au NPs, was placed at bottom, which was the front under front side illumination.

Figure 5 shows the characteristic electrochemical impedance spectra for DSSCs based on $TiO_2$ film and double layered $TiO_2$ film. The equivalent circuit is shown as the inset. One can see three semicircles in each spectrum. The hemisphere in the high-frequency region is assign to the parallel combination of the resistance and capacitance at the Pt-FTO/electrolyte and to the interface between FTO and $TiO_2$ layers, while those in the intermediate and low-frequency regions offer information on the resistance and capacitance at the $TiO_2$/electrolyte interface and the Nernst diffusion of the electrolyte, respectively.[24] One can see no significant difference between the two spectra. This may mean that a relatively low weight percent of Ag and Au NPs does not affect to the resistance and capacitance of the DSSCs.

In Figure 2(b), as the weight percent of Au NPs was raised up to 0.52 wt%, the $\eta$ value was gradually increased to the maximum value, 9.36%. A further increase of Au weight percent led to a steep decrease in $\eta$ and $J_{sc}$. This behavior is related to the plasmon-enhanced dye absorption and aggregation of metal NPs.[31] To prove it, we have studied the dependence of Au NPs weight percent on IPCE spectra of the DSSCs based on $TiO_2$/Au NPs film and N719 dye and based on $TiO_2$/Au NPs film and black dye (see Figure 6). For black dye, the IPCE values increase continuously with increasing the

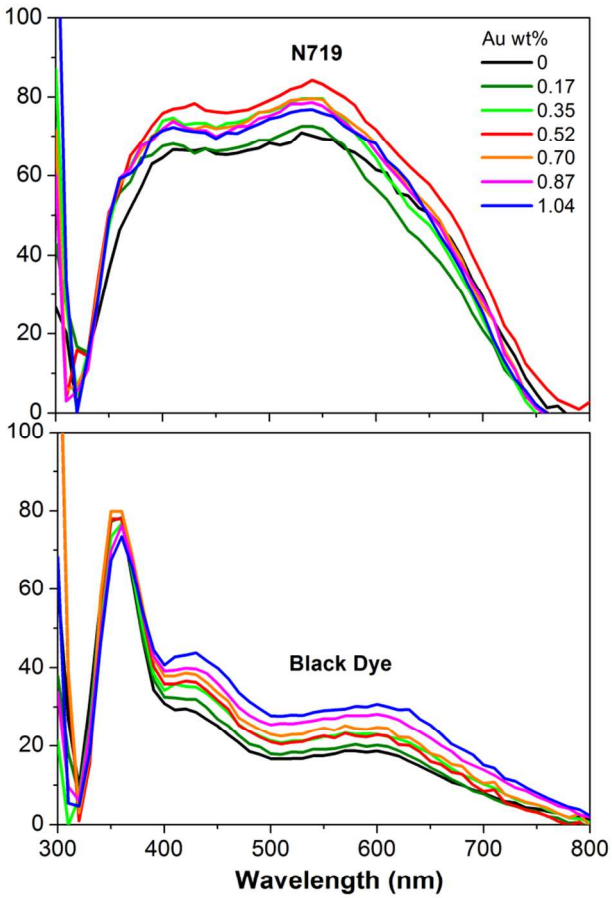


**Fig 6.** Dependence of Au NPs weight percent on IPCE spectra of the DSSCs based on $TiO_2$/Au NPs film and N719 dye (top) and $TiO_2$/Au NPs film and black dye (bottom). The average size of Au NPs included in the fabrication of the DSSC was 33 nm.

weight percent of Au NPs, while for N719 dye the values decrease steeply when the weight percent of Au NPs was increased further than 0.52 wt%. With increasing relative weight percent of Au NPs, the probability of aggregation between Au NPs in the composite films would be increased, and the concentration of the dimer of Au NPs might be increased. When Ag or Au NPs are aggregated, the resonance wavelength of the longitudinal mode is red-shifted.[29] The longitudinal mode of the monomer of Au NPs is centered at near 540 nm, while that of the dimer is centered at near 760 nm. N719 dye has two strong visible absorption bands centered at 393 and 533 nm, while black dye centered at 410 and 610. There is no doubt that the spectral overlap with black dye is much greater for the dimer of Au NPs than the monomer, while that with N719 is much lesser for the dimer than the monomer. The plasmon-enhanced absorption increases with increasing the spectral overlap between the localized plasmon resonance absorption of metal NPs and dye absorption.[31] Therefore, the IPCE values of the DSSCs based on based on $TiO_2$/Au NPs film and black dye could increase continuously with increasing the weight percent of Au NPs, while those of the DSSCs based on $TiO_2$/Au NPs film and N719 dye decrease steeply when the weight percent of Au NPs was increased further than the optimum weight percent, and the number of the dimer of Au NPs was

increased. This is clear evidence that the plasmon-enhanced absorption has taken place in our DSSCs included metal NPs. Also, it is suggested that the aggregation of metal NPs should be controlled to enhance the efficiency of the surface plasmon-enhanced DSSCs.

### Conclusion

We have fabricated N719 dye-sensitized solar cells based on double-layered films whose bottom layer consists of $TiO_2$ and Ag NPs, while the top one consists of $TiO_2$ and Au NPs. N719 dye, which is the most heavily used dye in DSSCs, has two strong absorption bands centered at 393 and 533 nm. The localized surface plasmon absorption of isolated Au nanoparticles is well matched with the longer wavelength band of N719 dye, while that of isolated Ag nanoparticles with the shorter one. The energy conversion efficiency of the DSSC based on double-layered film is 10.0%, which is almost the same as the highest value reported on the surface plasmon-enhanced DSSCs. The high efficiency may be due to a close optical matching between two visible absorptions of N719 dye and the localized surface plasmon resonances of Ag and Au NPs.

## Notes and references

Nano-materials Laboratory, Department of Chemistry, Seoul National University, Kwanakro 1, Kwanakgu, Seoul 151-742, Republic of Korea.
1 These authors contributed equally to the work.
*To whom correspondence should be addressed.
E-mail: jssuh@snu.ac.kr, FAX: 82-2-875-6636, Tel: 82-2-880-7763.

1. K. M. Mayer, J. H. Hafner, *Chem. Rev.* 2011, **111**, 3828.
2. M. Ihara, K. Tanaka, K. Sakaki, I. Honma, K. Yamada, *J. Phys. Chem. B.* 1997, **101**, 5153.
3. S. D. Standridge, G. C. Schatz, J. T. Hupp, *J. Am. Chem. Soc.* 2009, **131**, 8407.
4. A. Baba, K.Wakatsuki, K. Shinbo, K. Kato, F. Kaneko, *J. Mater. Chem.* 2011, **21**, 16436.
5. D. M. Schaadt, B. Feng, E.T. Yu, *Appl. Phys. Lett.* 2005, **86**, 063106.
6. D. Derkacs, S. H. Lim, P. Matheu, W. Mar, E. T. Yu, *Appl. Phys. Lett.* 2006, **89**, 093103.
7. S. Pillai, K. R. Catchpole, T. Trupke, M. A. Green, *J. Appl. Phys.* 2007, **101**, 093105.
8. J. L. Wu, F. C. Chen, Y. S. Hsiao, F. C. Chien, P. Chen, C. H. Kuo, M. H. Huang, C. S. Hsu, *ACS Nano*, 2011, **5**, 959.
9. S. P. Lim, A. Pandikumar, N. M. Huang, H. N. Lim, *RSC Adv.*, 2014, **4**, 38111
10. Y. Wang, J. Zhai, Y. Song, *RSC Adv.*, 2015, **5**, 210
11. J. L. Wu, F. C. Chen, Y. S. Hsiao, F. C. Chien, P. Chen, C. H. Kuo, M. H. Huang, C. S. Hsu, *ACS Nano*, 2011, **5**, 959.
12. J. W. Choi, H. Kang, M. W. Lee, J. S. Kang, S. Kyeong, J. K. Yang, J. Kim, D. H. Jeong, Y. S. Lee, Y. E. Sung, *RSC Adv.* 2014, **4**, 19851
13. W. Jiang, H. Liu, L. Yin, Y. J. Ding, *Mater. Chem. A,* 2013, **1**, 6433.
14. C. Hägglund, M. Zäch, G. Petersson, B. Kasemo, *Appl. Phys. Lett.* 2008, **92**, 053110.
15. S. D. Standridge, G. C. Schatz, J. T. Hupp, *Langmuir* 2009, **25**, 2596.
16. H. A. Atwater, A. Polman, *Nat. Mater.* 2010, **9**, 205
17. X. Zhang, J. Liu, S. Li, X. Tan, M. Yu, J. Du, *RSC Adv.* 2013, **3**, 18587.
18. I. K.; Ding, J. Zhu, W. Cai, S.-J. Moon, N. Cai, P. Wang, S. M. Zakeeruddin, M. Grätzel, M. L. Brongersma, Y. Cui, *Adv. Energy Mater.* 2011, **1**, 51.
19. M. D. Brown, T. Suteewong, R. S. S. Kumar, V. D'Innocenzo, A. Petrozza, M. M. Lee, U. Wiesner, H. J. Snaith, *Nano Lett.* 2011, **11**, 438.
20. Qi, J.; Dang, X.; Hammond, P. T.; Belcher, A. M. *ACS Nano,* 2011, **5**, 7108.
21. B. O'Regan, M. Grätzel, *Nature*, 1991, **353**, 737.
22. M. Grätzel, *Inorg. Chem.* 2005, **44**, 6841.
23. M. Grätzel, Nature, 2001, 414, 338.
24. Y. J. Kim, M. H. Lee, H. J. Kim, G. Lim, Y. S. Choi, N. -G. Park, K. Kim, W. I. Lee, *Adv. Mater.*, 2009, **21**, 3668.
25. S.-P. Ng, X. Q. Lu, N. Ding, W. C. -M. Lawrence, C.-S. Lee, *Sol. Energy* 2014, **99**,115–125.
26. H. Choi, W. T. Chen, P. V. Kamat, *ACS Nano*. 2012, **6**, 4418.
27. R. Asep, A. Isa, S. Akhmadi, I. Irman, *AIP Conf. Proc.* 2011, **1415**, 39.
28. N. C. Jeong, C. Prasittichai, J. T. Hupp, *Langmuir.* 2011, **27**, 14609.
29. S. Lee, G. H. Gu, J. S. Suh, *Chem*. Phys. Lett. 2011, **511**, 121.
30. U. Kreibig and M. Vollmer, *Optical Properties of Metal Clusters*, Springer Series in Materials Science, Springer, NY, USA, 1995.
31. H. -Y. Kim, W. -Y. Rho, H. Y. Lee, Y. S. Park, J. S. Suh, *Solar Energy* 2014, **109**, 61.

## Graphical Abstract

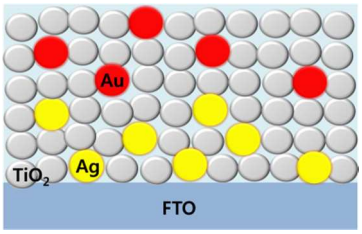


Double-layered composite films consisting of $TiO_2$/Ag and $TiO_2$/Au nanoparticles.